Hydrodeoxygenation of Guaiacol, A Surrogate of Lignin Pyrolysis Vapors, Over Iron Based Catalysts: Kinetics and Modeling of the Lignin to Aromatics Integrated Process

5 AUTHORS, INCLUDING:

Mohammed Bettahar
University of Lorraine
102 PUBLICATIONS **1,986** CITATIONS

SEE PROFILE

Anthony Dufour
French National Centre for Scientific Research
58 PUBLICATIONS **746** CITATIONS

SEE PROFILE

Hydrodeoxygenation of Guaiacol, A Surrogate of Lignin Pyrolysis Vapors, Over Iron Based Catalysts: Kinetics and Modeling of the Lignin to Aromatics Integrated Process

R. N. Olcese,[†] J. Francois,[†] M. M. Bettahar,[‡] D. Petitjean,[†] and A. Dufour[†,*]

[†]CNRS, Lorraine University, Reactions and Process Engineering Laboratory, ENSIC, 1, rue Grandville, 54000 Nancy, France
[‡]CNRS, Lorraine University, Faculté des Sciences et Techniques, SRSMC, bd des Aiguillettes, Vandoeuvre-les-Nancy, France

Ⓢ Supporting Information

ABSTRACT: Biosourced aromatics (BTX (benzene, toluene, xylene) and phenols) could be produced by lignin pyrolysis coupled with catalytic hydrodeoxygenation (HDO) of uncondensed pyrolysis vapors. Guaiacol is used as a model compound to study the catalytic HDO over Fe/SiO_2 catalyst. Experiments were conducted in a fixed bed reactor operated at 673 K (1 atm) with a gas mixture (guaiacol, H_2, H_2O, CO, CO_2) that mimics the real gas composition from lignin pyrolysis. Fe/SiO_2 catalyst was shown to be selective for guaiacol HDO into benzene and phenols because it does not catalyze the aromatic ring hydrogenation. Major and minor products are modeled by a semidetailed kinetic mechanism. A deactivation law is also determined. The kinetic model is then included in an Aspen Plus model of lignin to BTX process. Aspen Plus model handles (1) pyrolysis of lignin, including char, oligomers, gases and aromatic yields, (2) catalytic conversion of aromatics by the kinetic model, (3) heat exchangers, and (4) BTX vapors recovery by scrubbing with 1-methyl-naphthalene. Mass and carbon balances, heat demand, and selectivity in desired products are given for the overall process. The effect of gas dilution from pyrolysis reactor on BTX losses, heat demand, and scrubbing solvent flow rate is highlighted. High carrier gas flow rates (as required for biomass pyrolysis in fluidized bed) lead to the entrainment of fines and oligomers, dilute the products, and impact considerably the process intensification.

1. INTRODUCTION

Lignocellulosic biomass is seen as an interesting resource for green chemicals and fuel production. It is mainly composed of cellulose, lignin, and hemicelluloses. Cellulose is a useful polymer, with a well-developed market, while the conversion of lignin and hemicelluloses into fuel and chemicals is still being developed.[1,2] In one scenario of a future lignocellulosic biorefinery, cellulose and hemicelluloses would be depolymerized to be converted into ethanol and chemicals by fermentation, so generating considerable amount of lignin (~25 wt % of lignocellulosic biomass).[1,3]

Lignin is a very heterogeneous resource. Its composition and properties vary with biomass type, growing conditions and polymer fractionation process.[1,4] However, lignin is always composed of aromatic monomers with different fractions in guaiacyl, syringyl or coumaryl groups.[4]

Lignins are used to produce heat and power in the pulp and paper industry, but new valorization routes are needed to improve the economic picture of lignocellulosic biorefinery.[1,2] Lignin could be used to coproduce heat and power, a syngas, activated carbon,[5] carbon fibers,[6] aromatic hydrocarbons (BTX (benzene, toluene, xylene)),[7,8] fine chemicals (such as vanillin),[9,10] phenol,[11] phenolic resins,[12] etc.

Among those potential strategies, the present research work focuses on the development of processes for the conversion of lignin into aromatic hydrocarbons (BTX). The importance of this route has been outlined in literature.[1,3,4,7] Phenol is more expensive than BTX, and lignin to phenol strategies have also been considered.[3,11] Table 1 summarizes literature results on

proposed processes for the conversion of lignin into aromatic hydrocarbons. This nonexhaustive list shows different examples of the main routes considered. The main goal for all these processes is to conduct a selective removal of oxygen atoms from lignin by hydrodeoxygenation-HDO, dehydration, decarboxylation, etc. Furthermore, unpublished technologies may have been developed by private companies waiting for higher crude oil prices.[9,11,13] Results concerning lignin oxidation to high value-added chemicals (such as vanillin) were excluded. One can refer to Zakzeski et al.[4] for an exhaustive review of lignin valorization.

All processes have advantages and disadvantages (Table 1) and few of them have been optimized to their best. The process choice depends on the lignin source and on the desired products. For example, a process working in the liquid phase would be chosen for a liquid lignin (such as Kraft lignin), but pyrolysis would be more suitable for lignins with a low water content (evaporating high amounts of water would be energy-consuming). Lignin composition also affects the viscoelastic properties of the "sticky" intermediate material formed under heating, which could govern process design.[26] More research is needed to choose the best process for each lignin type.

The vapor phase HDO of uncondensed lignin pyrolysis vapors on a cheap and simple iron catalyst is our strategy based on previous works on biomass pyrolysis and HDO (Figure

Table 1. Some Processes (Not Exhaustive) for Lignin Valorization into Hydrocarbons

name and references	description	state of the art	pros	cons
"Noguchi Process"[11]	Catalytic hydrotreatment of lignin dissolved in a lignin-based phenolic mixture.	Many operating conditions were tested by Crown Zellerbach company, for the production of phenol and p-cresol, but they were judged nonprofitable in 1965.	High yields in monophenols, coproduction of nonoxygenates.	Expensive reactors for hydrotreatment at >400 °C, complex separation (distillation) of products.
"Catalytic ebullated bed"[14]	Lignin is introduced into a CoMo catalyst bed fluidized by boiling phenols, hydrogen being sparged through this ebullated bed. Volatile low oxygen content phenols (mainly cresols) are transferred to the gas phase and are condensed downstream of the bed.	A pilot was operated in 1980.	Mainly phenol and cresols are produced.	A carbonaceous solid is formed and the bed is easily clogged.
"Base catalyzed depolymerization and HDO of phenols"[7]	Lignin is treated by H_2O (catalyzed by NaOH) to yield phenols. The solution is neutralized and phenols are extracted, and then hydrotreated (50 bar H_2, transition metal catalyst).	In the demonstration stage (Chevron, ENI)[13]	High yield of hydrocarbons (64 wt % dry lignin)	Too many steps to separate phenols from reaction media.
"Catalytic Pyrolysis"[8,15,16]	Lignin is pyrolyzed in presence of a solid catalyst.	Pilots were operated based on FCC units.[16] Many catalysts have been optimized in a pyroprobe (1 mg scale). Researches are conducted to scale up laboratory experiments to a continuous pilot.	No need of hydrogen. Low pressure.	Lignin char is agglomerated with the catalyst, difficult regeneration and steady-state operation
"Pyrolysis, and HDO of condensed pyrolysis vapors"[17]	Lignin is pyrolyzed, vapors are condensed and then hydrotreated (100 bar H_2, precious metal catalysts).	A pilot was operated by De Wild et al.[17] (ECN Netherlands). Fluidized-bed clogging happened, but that may be solved by optimizing design.[7,18]	Phenols are separated from char before catalytic treatment	Low yield of hydrocarbons heavier than C_6.
"Pyrolysis and low pressure, gas phase HDO of uncondensed phenolic vapors"[19−25 and this work]	Lignin is pyrolyzed; vapors are hydrotreated before condensation.	After catalyst development with model compounds, experiments focus on real vapors.	Catalysts are not in contact with lignin/char. Easier operation of reactors. Low pressure. Cheap catalyst.	Need the development of a trustable steady-state lignin pyrolysis reactor with a high vapor yield.

1).[19,20,27,28] Gas-phase HDO prior to condensation would help to optimize heat integration of the process and reduce problems of feeding the reactive liquid bio-oils.
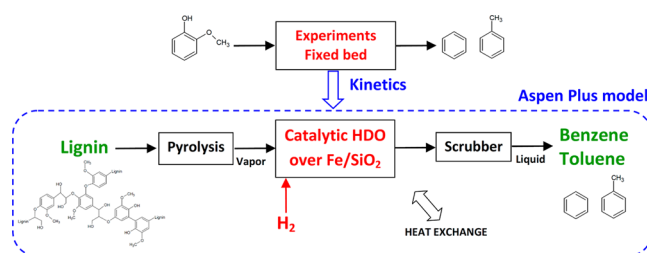

Figure 1. Scope and methodology presented in this paper: experiments on a model compound (guaiacol) are used to model the whole lignin to BTX process under Aspen Plus.

Other works have dealt with catalytic conversion of lignin pyrolysis model compounds in gas phase[21,29−32] and integration of a fixed bed after a (lignin or wood) pyrolysis reactor.[25,33,34]

The interest and selectivity of cheap and green Fe/SiO_2 has been previously presented and compared with other catalysts.[19,20] Other active phases suitable for gas phase and low pressure operation have also been recently identified (such as Pt/Al_2O_3,[35] $Pt-Sn$,[21] Ni_2P[23]). Iron-based catalysts were shown in pioneer work to exhibit some low activity for liquid-phase phenolic HDO.[11,36] Fe-based catalysts were also tested on wood pyrolysis vapors in the absence of H_2 (Fe/zeolites,[33] Fe/Al-MCM-41[37]), showing an effect of iron to convert methoxy-phenols.

In previous work,[19] the catalytic properties of Fe/SiO_2 were investigated for guaiacol HDO (in H_2) as a function of temperature and H_2 partial pressure (etc.). The mechanism of guaiacol HDO over Fe/SiO_2 was discussed. Coke deposit was also investigated by temperature programmed oxidation. In a second article,[20] the effect of gas composition during guaiacol HDO on catalyst deactivation, iron speciation (by XRD and Mössbauer analysis), and coke deposit (by temperature programmed oxidation and high resolution TEM) was studied.

The scope of the present paper is illustrated in Figure 1. Experimental data presented here are obtained for guaiacol conversion in a more complex mixture (H_2, H_2O, CO, CO_2, i.e., approaching real process conditions) as a function of the mass of catalyst (by keeping gas flow rate constant). The data are used in order to develop a kinetic model for guaiacol HDO. Then, this semidetailed kinetic model is included in an Aspen Plus process model (see Figure 1), using data from de Wild et al.[17] for lignin pyrolysis. Process aspects on coupling pyrolysis, catalytic reactor, and aromatic compound recovery are discussed.

2. EXPERIMENTAL AND KINETIC MODEL

The detailed experimental procedure has been previously described.[19,20]

15% Fe/SiO_2 was prepared by simple vacuum impregnation of fumed silica (Aerolyst 3039) with a water−iron nitrate nonahydrate solution (Sigma). It was dried, calcined, and reduced in situ (before guaiacol HDO) at 773 K under H_2. Table 2 summarizes the properties of 15%Fe/SiO_2 catalyst.[20]

The setup used for the catalytic experiments (presented in the Supporting Information) is based on a differential fixed bed reactor. A mixture of 50% H_2, 5% CO_2, 2.5% CO, 2.5% H_2O, 1% guaiacol (balance argon) was prepared by using four mass flow controllers and

Table 2. Properties of Catalyst (15%Fe/SiO$_2$) Employed in This Work (from ref 20)

iron loading (wt %)	14.7
specific surface (m^2/g)	144
apparent density (kg/m^3)	396
catalyst particle size (μm)	100−380
iron particle size (nm)^a	17

^{a}Crystallite size measured by Scherrer's equation based on XRD analysis, checked by TEM.

two syringe pumps. Reactive stream was injected over the catalyst in a fixed bed reactor through a heated line (see Supporting Information). The total flow rate was 45 N mL/min and kept constant between tests. The mass of catalyst was changed (58−1034 × 10^{-6} kg$_{cat}$) to study the kinetics of the reaction. Experiments were conducted at 673 K and atmospheric pressure.

Products were sampled through a heated line to a Gas Chromatography-Flame Ionization Detector (GC-FID, 1701 column) with a heated loop (508 K). The exit of the sample loop was connected to two impingers at 273 and 213 K filled by 2-propanol. Liquid injection was used to check the results from online GC-FID through internal calibration and liquid injection GC/MS-FID analysis.[19] Noncondensable gases were analyzed at the outlet of impingers by a Varian 490 μGC equipped with four modules. More details on the analytical procedure can be found in refs 19 and 20. Areas from GC-FID analysis were converted into concentration using experimental response factors. Molar flow was calculated considering no gas phase volume expansion. Data was fitted by the kinetic model using an Excel solver.

It has been previously shown that the conversion rate of guaiacol was not limited by internal and external mass transfer diffusions through modified Thiele (Weisz) modulus calculation and flow rate variations.[19]

3. DEFINITION OF ASPEN PLUS MODELING

Our group has previously developed models under Aspen Plus for gasification processes by coupling pyrolysis correlations with kinetic mechanisms.[38,39] The goal of this work is to give a simplified but realistic model to assess process integration and operating variables. Figure 2 depicts a scheme of the lignin to BTX process modeled under Aspen Plus.

To the best of our knowledge, such an integrated model, which couples the description of lignin pyrolysis with lumped compounds and a semidetailed kinetic mechanism for catalytic HDO, has never been previously developed.

More details on the block units (input and output) and the Aspen Plus flow sheet are given in the Supporting Information.

Redlich−Kwong−Aspen (RK-ASPEN) was used as the thermodynamic property method for conventional compounds. All Aspen Plus process units are operated at atmospheric pressure.

3.1. Definition of the Components: Lignin, Char, Lignin Oligomers, and "PYROLOST". Lignin, lignin oligomers, and char were treated as in Aspen Plus as "nonconventional solids" (Aspen Plus terminology). All other compounds were defined as conventional compounds in the Aspen Plus database. Lignin was considered to be 57.8 wt % C, 5.7 wt % H, and 36.5 wt % O (that corresponds to an oxygenated lignin[40]). Fixed carbon was 40% and volatile matter 60%.[17] It is assumed dry and ash-free for Aspen Plus simulation. Char was considered to be 72.4 wt % C, 4.5 wt % H, and 23.1 wt % O[41] with 100% fixed carbon. Lignin's oligomers (∼10 wt % yield from dry lignin) were considered to be only one lumped compound and the formula was taken from Scholze et al.[42] The formula assumed for lignin oligomers is CH$_{0.9}$O$_{0.2}$ (model A in ref 42). Fixed carbon and volatile matter were assumed the same as lignin. The enthalpies of the three nonconventional solids were predicted based on the HCOALGEN Aspen property model. For lignin, the heat of combustion was set to 23260 kJ/kg,[1] while it was calculated from Boie's correlations for lignin oligomers and char. Heat capacities were calculated from the Aspen Plus built-in Kirov's correlation. The density of lignin, char, lignin oligomers, and PYROLOST were predicted with DCOALIGT built-in tool. The relevancy of HCOALGEN, Boie's correlation, and DCOALIGT models has been previously discussed.[38,43]

A theoretical compound, called PYROLOST, was introduced to close the atomic balance for pyrolysis. It was defined as a nonconventional solid, fixed carbon 10%, volatile matter 90%, 94.4 wt % C, and 5.6 wt % H. Enthalpy calculations were also based on HCOALGEN method.

3.2. Modeling of Lignin Pyrolysis Products. Lignin pyrolysis was modeled based on data from de Wild et al.[17] These authors operated a fluidized bed at 673 K and 0.1 kg/h of lignin. This work was selected because of the pertinence of the experimental design (flash pyrolysis in an adapted fluidized bed) and the analytical tools leading to a good mass balance (89%). Lignin pyrolysis produces many compounds that cannot be analyzed by GC. For that reason, experimental mass balance is always deficient.

The lignin input flow is fixed to 500 kg/h in the simulation that could correspond to a demonstration unit scale.[44]

Lignin pyrolysis aromatic vapors (∼9 wt %) were considered to be only guaiacol. Guaiacol is assumed to be a "lumped" model molecule representative of functional groups in aromatic vapors. In future development of the model, other lumped species could be defined (as in ref 38) if kinetic data on their catalytic HDO are available. Traces of acetic acid and dimethyl-ketone were also considered to model light oxygenated hydrocarbons. As a consequence of lumping aromatic vapors into guaiacol and experimental uncertainty, atomic O balance
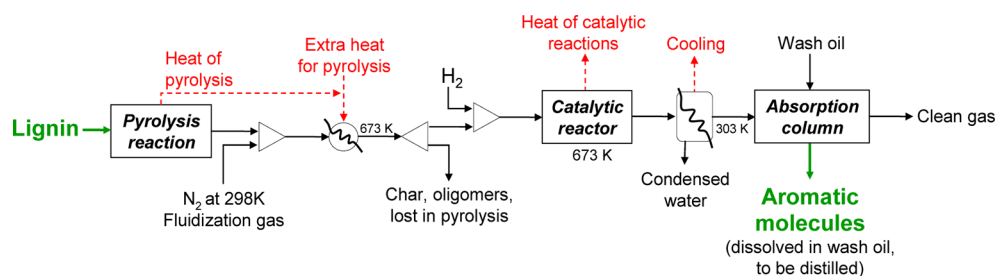

Figure 2. Scheme of Lignin to BTX process by HDO of pyrolysis vapors and its simplification for modeling under Aspen Plus.

Table 3. Comparison between Lignin Pyrolysis Experimental Data (Mass Fraction) Taken from Ref 17 and Data Introduced in Our Model

real compound	% wt measured by De Wild et al.[17]	model compound	% wt introduced in Aspen Plus simulation
char	30	char	30
H_2O	21	H_2O	14.18
unknown condensable products	12	assumed as a lignin-oligomer, molecular structure taken from Scholze et al.[42] (Model A: $CH_{0.9}O_{0.2}$)	12
phenols (guaiacol, syringol, alkyl phenols, etc.)	9	guaiacol	9
noncondensable gases	17[a]	CH_4	1.46
		CO	3
		CO_2	12.54
methanol	2.18[a]	methanol	2.18
other hydrocarbons (acetone, formic acid, furaldehyde)	0.1−0.2[a]	acetic acid	0.2
		acetone	0.2
lack in mass balance (pyrolysis loss)	11	PYROLOST	15.24

[a]Distribution of noncondensable gases, methanol, and other hydrocarbons yields taken from different experimental conditions (batch pyrolysis experiment at 773 K, from ref 17) than other ones (continuous fluidized bed at 673 K). These experimental yields are given for a sake of comparison with the data included in the model, but methanol and other hydrocarbons (2.18 wt % and 0.2 wt %) are not included in the experimental mass balance closure (100 wt % without methanol and other hydrocarbons).

exceeds 100%. Hence, the water yield was decreased until O balance close perfectly. We choose to change water yield rather than other oxygenated products for three reasons: (1) it does not change the carbon yield, which is a very important parameter in this work and for process selectivity, (2) water is produced in a high amount and closure of O balance has few effects on its overall yield, and (3) H_2O molar fraction has few chemical effect on kinetics of tar HDO in this range of variation.[20]

The mass yield in oligomers was kept from ref 17, and the molecular structure was taken from Scholze et al.[42] The char yield[17] and the elemental formula[41] were also fixed.

The PYROLOST compound was thus defined to close C and H balances. The closure of C and H balances leads to a formula $CH_{0.7}$ which is consistent with a loss as "soot" or heavy PAH that could be formed in the gas phase conversion of primary tar and/or from char fines entrainment. It is a simplified assumption because the pyrolysis loss could be also composed of oxygen, but we previously explained the reasons to change water yield rather than other products to equilibrate atomic O balance.

Table 3 sums-up the experimental data taken from De Wild et al.[17] and the data introduced in Aspen Plus model.

3.3. Operating Blocks and Flow-Sheet. The modeled and simplified lignin to BTX process is composed of a pyrolysis reactor, heater of pyrolysis products, and carrier gas (to simplify the model of pyrolysis reactor), catalytic reactor, condenser, and absorber for BTX recovery (see Figure 2). The detailed input and output for each process unit are provided in the Supporting Information.

We are aware that many more process steps are needed[45,46] and that stage condensation could help increasing the BTX yield.[45,47]

a. Lignin Pyrolysis Reactor. Lignin pyrolysis was modeled by a reactor with fixed yields of products (by a "RYield reactor" in Aspen Plus). Pyrolysis product yields are set from the experimental results defined in Table 3. The pyrolysis reactor operates isothermally at 298 K to simplify the model. The fast pyrolysis reactors obviously operate at higher temperature (673−773 K). Heat effects and temperature of the pyrolysis reactor are correctly captured by a subsequent heater block in

the model. This assumption is used to simplify heat integration in Aspen Plus, otherwise much complex modeling method should have been used, as in ref 38. Heat is generated as lignin pyrolysis is globally an exothermic reaction due to cross-linking reactions competing with bonds cleavage during lignin pyrolysis.[40,48] Heat of pyrolysis is calculated by Aspen Plus from the enthalpy of lignin and products.

Lignin pyrolysis products are then mixed with N_2 at 298 K (carrier gas used for fluidized bed reactor). This mixture is then heated up to 673 K (temperature of the pyrolysis reactor), using the heat produced during pyrolysis and some extra needed heat.

Char, lignin oligomers, and PYROLOST are then separated from the gaseous mixture with a 100% split fraction (modeled with a "Sep block" under Aspen Plus). In real conditions, some of these products stay in the fluidized bed and the downstream train.

b. Hydrogen Mixing. Hydrogen is heated to 673 K and mixed to pyrolysis products. The H_2 flow rate is calculated to ensure that $H_2/(H_2 + H_2O)$ ratio is an iron-reducing gas (taking into account H_2O produced by lignin pyrolysis and HDO). This condition is needed to maintain the activity of the catalyst.[20]

c. Catalytic Reactor. The catalytic reactor was model as a plug flow reactor (by an Aspen Plus "RPlug" reactor). Kinetics from experimental data were introduced in this catalytic plug flow reactor (see Figure 1). A detailed thermodynamic approach has been presented previously, showing that the reactive system is not limited by the thermodynamic equilibrium but by the kinetics.[19]

To overcome discontinuities due to zero order reactions in the kinetic mechanism (justified hereafter), a combination of three RPlug reactors in series was implemented (see the Supporting Information). Indeed, with zero order reactions, Aspen Plus calculates the reactions even if the reactive components are totally consumed. In the first reactor, the mass of catalyst is defined to have guaiacol conversion so the guaiacol exit flow is less than 0.01 kg/h. In the second reactor, guaiacol reactions are not considered and the mass of catalyst is defined so that methanol mass flow is less than 0.01 kg/h. In the third reactor, methanol reactions are not considered and the

mass of catalyst is adjusted so that phenol exit mass flow is 0.1 kg/h. Phenol is a more stable intermediate compound than guaiacol and methanol (see the kinetic results). That is why the exit mass flow was set to a higher value for phenol (0.1 kg/h) to narrow the size of the catalytic reactor. The combination of the three RPlug reactors represents the HDO reactor, and it results in 650 kg of catalyst based on our kinetic data. 650 kg of catalyst for 500 kg/h of lignin gives a WHSV (weight hour space velocity), defined as the biomass flow rate divided by the mass of catalyst of around 0.8 h^{-1}, which is similar to experimental data on wood pyrolysis vapors conversion over zeolite catalyst.[49] In real biorefinery conditions at commercial scale, the conversion would be adjusted to match with desired products and with catalyst deactivation. The deactivation of catalyst is not included in this Aspen Plus model. Deactivation and regeneration cycles in sequential reactors have to be further experimentally studied (on real lignin pyrolysis gas) and modeled.

Catalytic coke was modeled by C(s) graphite, that is a conventional solid in Aspen Plus. Carbon deposit exhibits a very different structure from graphite, but the latter was chosen to simplify the model. Heat (calculated by Aspen Plus from enthalpy of input and output compounds) is generated in the HDO reactor since HDO reactions are exothermic[19] and that isothermal conditions are required.

d. Separation of Products and Cleaning of Gas Phase. Catalytic coke was separated from product stream (with a separator under Aspen Plus). In real conditions, coke remains on the catalytic material.

Coke free products were cooled to 303 K (see Figure 2). Condensed products at 303 K were separated in a single stage column performing gas–liquid phase equilibrium calculations (modeled with a "Flash2 block" in Aspen Plus).

The liquid-free product stream was injected to the bottom of the scrubber modeled as an absorption column (by a "RadFrac block" under Aspen Plus) with 5 theoretic plates to model the absorption of BTX by 1-methylnaphthalene. The RadFrac block represents a simplified model of the absorber based on the known process to recover BTX in coal carbochemistry plants.[46] It is out of the scope of the present article to give a detailed model description of the BTX absorption and recovery process. 1-Methyl naphthalene was introduced to absorb gas in the RadFrac block. The UNIFAC method was used to predict thermodynamic equilibrium in the absorption column (i.e., activity of compounds at the liquid phase vs partial pressure at gas phase). The UNIFAC method is recommended to predict the thermodynamic properties of hydrocarbons.[50] The 1-methyl naphthalene flow rate was varied until the benzene recovery reached 97%, in agreement with the recovery efficiency in industrial carbochemical processes.[46]

4. RESULTS

4.1. Reaction Pathway and Kinetics of Guaiacol HDO over Fe/SiO$_2$ Catalyst.
In Figures 3 and 4, the molar flow rates of guaiacol and products at the exit of the experimental fixed bed reactor are displayed as a function of the mass of catalyst for 67 min time on stream. The reactor was operated for 3 h. The effect of time on stream on kinetic rates is discussed in the next section. Molar flow rates of guaiacol and products as a function of time on stream for all the catalyst masses are given in the Supporting Information.

Figure 5 shows the proposed reaction pathways for guaiacol HDO over Fe/SiO$_2$ based on the evolution of products as a
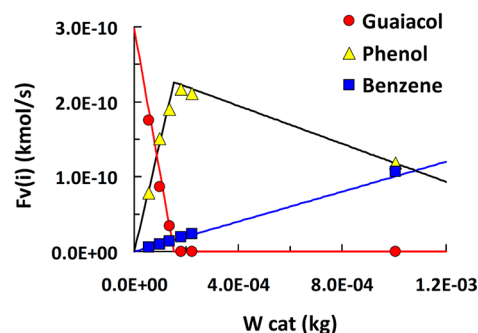

Figure 3. Effect of catalyst mass on guaiacol and major products (benzene, phenol) molar flow rate (15% Fe/SiO$_2$ at 673 K, after 67 min time on stream). Points are experimental data, lines from the kinetic model.
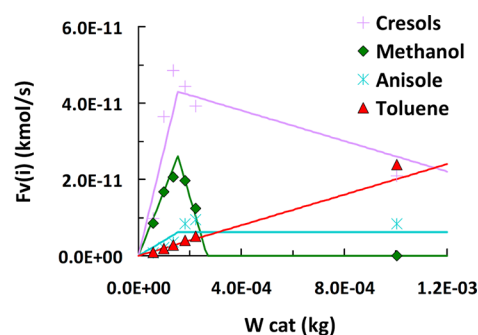

Figure 4. Effect of catalyst mass on flow rate of minor products. (15% Fe/SiO$_2$ at 673 K, after 67 min time on stream). Points are experimental data, lines from the kinetic model.
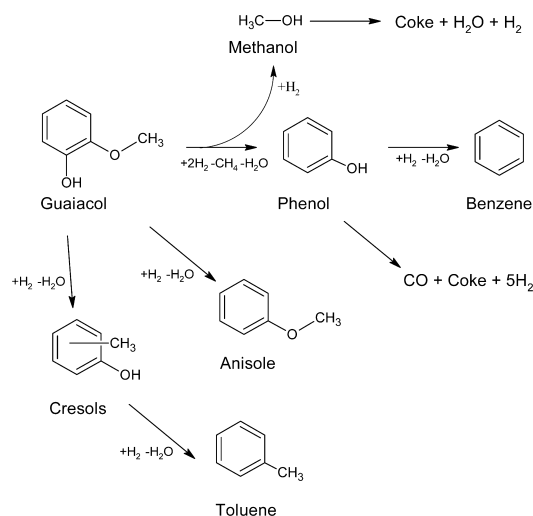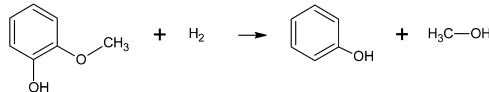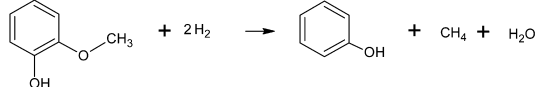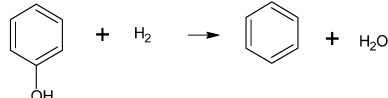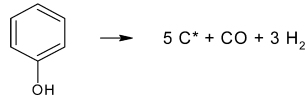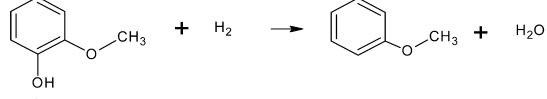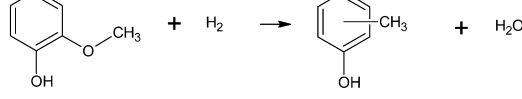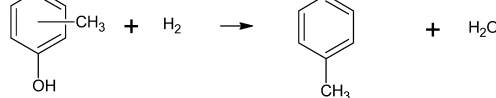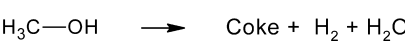

Figure 5. Proposed pathways for the HDO of guaiacol over Fe/SiO$_2$.

function of the mass of catalyst (Figures 3 and 4). Guaiacol is converted mainly into phenol, but some anisole and cresols (the sum of three isomers) are also produced. Phenol is further converted into benzene. Anisole seems to be stable in our conditions. Toluene is formed from cresols. Methanol exhibits a maximum and then decreases. The amount of produced methanol (only 10% vs produced phenol, see Figures 3 and 4) is too low to be explained solely by the decomposition of guaiacol into phenol. Therefore, we proposed that guaiacol is converted to phenol by two reaction pathways in Figure 5: pathway-1, by producing CH$_4$, H$_2$O (i.e., consuming two H$_2$

Table 4. Kinetic Constant (k_i) for Guaiacol HDO Obtained from Experimental Data[a] Using a Zeroth Order Model for All Reactions

Reaction	k_i (kmol s^{-1} kgcat^{-1})
	4.0E-07
	1.2E-06
	1.1E-07
	2.1E-08
	4.0E-08
	3.0E-07
	2.4E-08
$H_3C\!-\!OH \longrightarrow$ Coke + H_2 + H_2O	2.3E-07

[a]1 atm, 673 K, 15% Fe/SiO$_2$ catalyst, 50% H$_2$, presence of CO, CO$_2$, H$_2$O, presented in Figures 3 and 4, after 67 min time on stream.

molecules), and pathway-2, by producing methanol (and phenol) and consuming only one H$_2$ molecule. When the mass of catalyst is high and guaiacol completely converted, methanol concentration decreases sharply. We explained this evolution by the conversion of methanol, which is no longer supplied by guaiacol HDO (pathway-2). The conversion of methanol does not result in an increase of CH$_4$ (see Supporting Information), so methanol cracking into CO, H$_2$, and coke was proposed. The molar balance of aromatic rings was closed at 90−95%. This loss in aromatic rings could be explained by phenol cracking into H$_2$, CO, and a carbonaceous deposit. More details on the chemical mechanism of guaiacol HDO over Fe/SiO$_2$ can be found in ref 19.

The apparent rate of a compound i decomposition (or formation if the sign − in eq 1 is replaced by +), expressed per unit mass of catalyst, r (kmol s^{-1} kg$_{cat}^{-1}$), reads:

$$r = -kP_i^n = -k(RT)^n C_i^n \tag{1}$$

where n is the reaction order, k is a kinetic constant (kmol s^{-1} kg$_{cat}^{-1}$ atm^{-n}), P_i is the partial pressure of reactant i, R is the molar gas constant (8.205×10^{-2} m^3 atm kmol^{-1} K^{-1}), T is the temperature of the catalyst bed (K), and C_i is the molar concentration of i in the gas phase (kmol m^{-3}).

Assuming plug flow for the gas phase flow across the catalyst bed, the molar differential balance of i over a catalyst mass dm, of an elementary slice of the bed, reads

$$dF_i = -k(RT)^n \left(\frac{F_i}{Q} \right)^n dm \tag{2}$$

where F_i is the molar flow rate of the converted compound (kmol s^{-1}) and Q is the total volume flow rate of the gas phase (m^3 s^{-1}) at the temperature of the reactor and at atmospheric pressure.

Integration of eq 2 for $n \neq 1$ leads to eq 3.

$$\frac{1}{1-n}(F_i^{1-n} - F_{0i}^{1-n}) = -\frac{k(RT)^n}{Q^{n-1}}t \tag{3}$$

where F_{0i} (kmol/s) is the molar flow rate at the entrance of the catalyst bed and t (s kg$_{cat}$ m^{-3}) is the space time.[51]

From eq 3, it can be demonstrated that when the molar flow rate of a compound (product or reactive) exhibits a linear evolution with the mass of catalyst (or space time) the apparent reaction rate can be assumed zeroth order.

Linear evolutions are observed for guaiacol, benzene (Figure 3), and toluene (Figure 4) as a function of the catalyst mass. Intermediate products (phenol, cresols, methanol, anisole) also showed linear evolution during their formation from guaiacol conversion, followed by linear decrease (for phenol, cresols, and methanol) after the complete conversion of guaiacol. Consequently, zero order kinetic for all reactions was assumed and experimental data was fitted this way. The apparent zero order kinetics observed for all reactions would indicate that the oxygenated species are strongly adsorbed through hydroxyl moieties with a high surface coverage.[52−54] The development of a more detailed kinetic model is out of the scope of this article. The aim of this work is rather to determine the apparent rates of the main reactions under conditions of high BT yield

production and to implement these apparent rates in the Aspen Plus model.

Table 4 shows the kinetic constants determined for each reaction. This data was used to model the evolution of compounds as a function of catalyst mass presented in Figures 3 and 4. Discontinuities are produced by the zeroth order model (when a reactant disappears, the reaction stops).

The kinetic constants presented in Table 4 (obtained at 67 min time on stream) are those used in the Aspen Plus simulations. The highest conversions with a constant gas composition at the outlet of the fixed bed reactor (see Supporting Information) are obtained at this value of time on stream. We are aware that initial conversion values (calculated by extrapolating data to zero time on stream) are often used to analyze catalyst performance prior to significant deactivation.[35] While kinetic studies at initial and low conversions are suitable to analyze the fundamental kinetics on fresh catalyst, they are not of practical interest to predict the rates of desired products formation at a significant yield and on a partially deactivated catalyst. That is why the experiments are conducted with a broad range of catalyst mass, including high guaiacol and phenol conversions. As shown previously,[19,20] it is of paramount importance to conduct experiments at high conversions. Such experiments are needed to demonstrate that the catalysts are really selective for benzene and toluene productions in a significant yield.[19,20]

Indeed, at high conversions, some catalysts could promote the hydrogenation or cracking of aromatic rings, becoming not selective for benzene production. This does not happen with iron because it preserves the aromatic ring.[19,20] For this reason, we proposed to plot the selectivity in benzene and toluene yield as a function the $C_{aromatic}$−O bond cleavage.[19] Figure 6 depicts

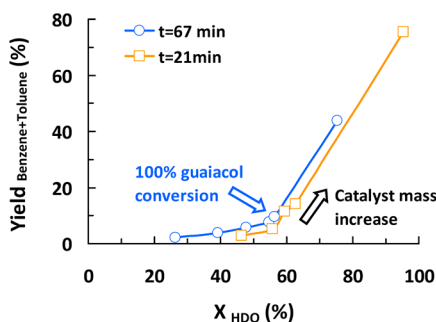**Figure 6.** Yield in benzene and toluene as a function of $C_{aromatic}$−O bond cleavage (X_{HDO}) as a function of the mass of catalyst used and for two times on stream (21 and 67 min). See ref 19 for more details on yield and X_{HDO} calculations. For one time on stream, each point corresponds to different catalyst masses (presented in the Supporting Information, Figure S.2). The selectivity in benzene and toluene should be proven at high HDO conversion, in such a diagram, to demonstrate that the catalysts are really selective for benzene and toluene productions in a significant yield. A very good selectivity is obtained with iron supported over silica.

this diagram for the results presented in Figure S.2 in the Supporting Information. Such a diagram should be used to compare catalysts activity and selectivity for similar operating conditions.[19]

From Figure 6, it is important to notice that the deactivation does not modify the shape and slope of the curve (BT yield vs X_{HDO}), so the deactivation does not affect the selectivity of the catalyst.

4.2. Catalyst Deactivation.
Catalyst deactivation was observed, as is inherent to this type of reactions for all types of catalysts due to coke formation.[19,21]

During 187 min of time on stream, the distribution of products changed (see the Supporting Information). Independently of the mass of catalyst used (58−1034 × 10^{-6} kg), the products were more oxygenated at the end than at the beginning. The experimental point at 21 min (in the Supporting Information) exhibits a particular behavior that is related with the stabilization of pseudo-steady-state of adsorbed molecules on the catalyst surface, so it was not considered in kinetic calculations. The same zero order model was applied to points at different time on stream. The values of kinetic constant of selected reactions vs time on stream are plotted in Figure 7. Among empirical laws for coke-induced catalytic
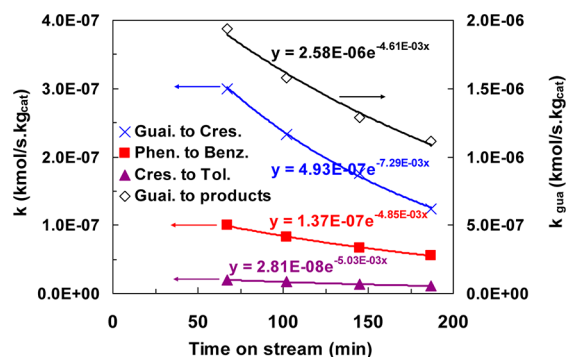
Figure 7. Decrease of kinetic constants along time on stream for some reactions, based on zero order model and experimental results (given in the Supporting Information). Reactions (reactives and products) are presented in Figure 5. The first points at 67 min corresponds to the kinetic data given in Table 4. "Guaiacol to products" accounts for the global rate of guaiacol conversion.

deactivation,[55] $k = k^0 \exp(\alpha t)$ was found to best fit all the data. k is the reaction rate in kmol s^{-1} kg^{-1}, k^0 is the initial reaction rate, α is the deactivation coefficient in min^{-1}, and t is the time on stream in minutes. The mechanism of catalyst deactivation (from coke deposit and iron oxidation) has been previously discussed based on temperature programmed oxidation, N$_2$ sorption, XRD, and Mössbauer spectroscopy analysis of catalysts.[19,20] Mössbauer analysis of the fresh and spent catalysts is discussed in Supporting Information.

α was between 4.6−5.03 × 10^{-3} min^{-1} for all curves except for guaiacol to cresol reaction (Figure 7). This could mean that all reactions are taking place over similar active sites that deactivate roughly at the same rate. Active sites may be in the vicinity of iron particles, where H$_2$ dissociation occurred, and SiO$_2$ support where molecules are adsorbed and react with dissociated H species.[19,20] The inhibition of the guaiacol to cresol reaction is fast. This reaction (that implies trans-alkylation) may happen on a different site.

4.3. Mass and Carbon Balances of Lignin to BTX Process Predicted under Aspen Plus.
All heat and mass flows predicted by our Aspen Plus simulation are listed in the Supporting Information. In the present paper, two process aspects are studied: (1) the mass and carbon yield of the whole process and (2) the effect of fluidization−dilution gas on process parameters.

Figure 8 displays the mass flows obtained from Aspen Plus model (besides N$_2$ and 1-methyl naphthalene). It can be pointed out that the amount of catalytic coke is relatively low
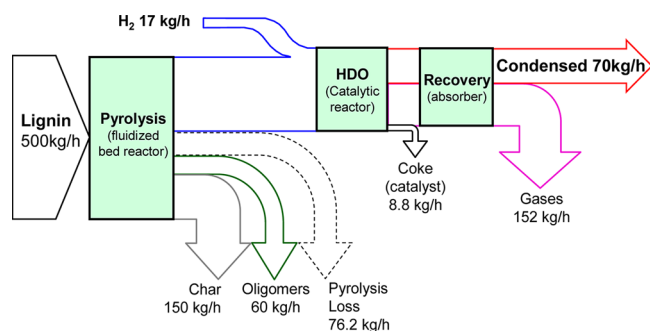
Figure 8. Mass flows from Aspen Plus simulation of the lignin to BTX process. N_2 (7200 kg/h) and 1-methyl naphthalene (14.4 m³/h) (Wash oil for recovery) are not represented. The 70 kg/h of condensed species are composed of 43.9 kg/h of water, 17.8 kg/h of benzene, and 4.3 kg/h of toluene (rest: methanol, cresols, etc).

compared with char, oligomers, and pyrolysis loss, which lead to the major loss in mass and carbon.

The "gases" output in Figures 8 and 9 represent both noncondensable gases (CO_2, CH_4, H_2, CO) and low amounts of condensable molecules (H_2O, benzene, etc) that are entrained in the N_2 flow.
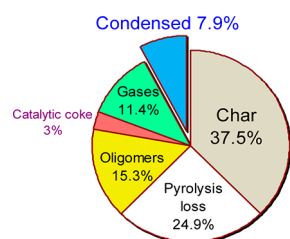

Figure 9. Lignin-based carbon yield of Lignin to BTX process by pyrolysis and gas-phase hydrotreatment at standard conditions (650 kg of catalyst for 500 kg/h of lignin, 7200 kg/h of N_2 carrier gas for pyrolysis reactor). Condensed benzene + toluene account for 7.5% C.

Condensable products are mainly water (43.9 kg/h), benzene (17.8 kg/h), toluene (4.3 kg/h), and other compounds not converted by the catalytic reactor (650 kg), because the mass of catalyst was set only to match with a 0.1 kg/h of phenol flow rate. If phenol becomes the desired product from lignin-derived pyrolytic vapors HDO over Fe/SiO_2, the mass of catalyst would be reduced from 650 kg (for 500 kg/h of dry lignin and to reach 0.1 kg/h of phenol if BTX are the desired products) to 52 kg to reach the maximum phenol yield (see the Supporting Information).

Figure 9 shows the distribution of carbon yields in the different streams. The char + oligomers + PYROLOST account for 77.7% of carbon atoms from lignin, while the yield of benzene + toluene is only 7.5% C (4.4% weight basis of dry lignin). The species condensed by the scrubber, which are not aromatics (acetone, acetic acid), represent only 0.4% of carbon.

The loss in carbon by the catalytic conversion or scrubber is very low compared with the carbon loss from the pyrolysis reaction. A more efficient pyrolysis technology is needed to obtain higher yields in volatile oxygenated aromatic compounds that can be further converted into chemicals.

The pyrolysis loss represents a substantial amount of missing carbon, 3 times (24.9% on lignin carbon yield) as much as the desired product (7.5%). An important loss in carbon, not converted into desired products, can be also attributed to

oligomers (15.3%). Our recent analysis by high resolution mass spectrometry on the HDO of real lignin pyrolysis vapors showed that heavy oligomers are not converted into desired products but into carbonaceous deposit over the catalyst.[56] The activity of the catalyst for the HDO of light aromatic compounds (lumped by guaiacol in the model) should be lower in a real pyrolysis gas than the predicted one (based on a model gas conversion) due to this carbonaceous deposit. Consequently, the yield in desired products obtained from lignin experiments would most probably be lower than the predicted one.

4.4. Effect of the Fluidization Gas Flow Rate on the Process Conditions. An important issue related to the pyrolysis in a fluidized bed is the dilution of lignin pyrolysis gases in the high molar fraction of N_2. The effect of the N_2 flow rate on selected process variables is plotted in Figure 10.
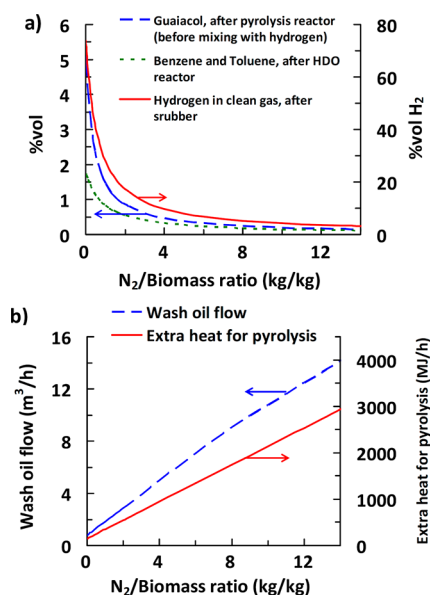

Figure 10. Effect of carrier gas flow rate over biomass flow rate used for pyrolysis on (a) gas phase composition (guaiacol, H_2, and benzene % mol) and (b) Wash oil flow rate and extra heat demand (heat of pyrolysis is not included).

An important N_2 flow rate must be heated for fluidization and furthermore electricity consumption of the blower should be taken into account. The heating could be carried out (in part) by heat recovery from the "cooling service" from the condensers (Figure 10), though a higher heat power to be recovered will be associated to higher investment cost in heat exchanger.

Another indirect variable is the flow of nonvolatile solvent (1-methyl naphthalene) needed to recover the desired products. As a fixed number of theoretic plates (5) was assumed in the simulation, a larger solvent flow will result into a larger absorption column. The aromatic loss is not increased by the dilution because the specification for the scrubber was set to 97% of benzene recovery. Indeed, the Wash oil flow rate is set by this specification and consequently increases with dilution.

When the flow rate of carrier gas increases, partial pressure of aromatics decreases and benzene is not condensed (in the condenser before the scrubber) from 7 N_2/biomass flow rate (kg/kg). When benzene is recovered in the condenser, the mass flow rate of benzene to the scrubber is reduced and the 97%

recovery specification is harder to reach because the partial pressure of benzene becomes lower. For that reason, a change in the slope of the Wash oil curve is observed near 7 kg N_2/kg $_{lignin}$. The product mixture at the exit of the catalytic reactor is condensed when cooled at 303 K (before entering in the absorber). However, when the N_2 flow becomes higher than 7 kg N_2/kg $_{lignin}$, the partial pressures are too low to condense the products, even at 303 K.

An important fraction of hydrogen does not react in the catalytic reactor. Figure 10 also shows the fraction of H_2 in the cleaned gas stream. An excess of fluidization gas will impede the separation of H_2 for recovery and recycling.

Fe/SiO_2 catalyst is active in the presence of pyrolysis gases. However, if the clean gas is recycled without CO_2 separation, the CO_2 partial pressure would increase in the pyrolysis and catalytic reactor and the gas mixture could become an iron oxidizing mixture. So, Fe/SiO_2 will be transformed into Fe_3O_4/SiO_2, and its activity would be decreased.[20]

For all these reasons, it would be advantageous to decrease the fluidization gas flow rate as much as possible, which depends on particle class and fluidization regime.[57]

Using H_2 as fluidization gas could solve some of these issues, but it would lead to safety problem and a high consumption in H_2 if not recycled.

Furthermore, other technologies of pyrolysis reactors with a lower need in carrier gas flow rate could be looked for.[18,58]

5. CONCLUSION

Lignin conversion to aromatic hydrocarbons by direct HDO of pyrolysis vapors is a potential strategy for the valorization of dry lignin.

Experiments in a fixed bed reactor on a model compound (guaiacol) HDO over Fe/SiO_2 catalyst are used to develop a semidetailed kinetic mechanism and to assess catalyst deactivation. The kinetic mechanism involves eight reactions with zero order kinetics. A deactivation law is proposed. It is shown that the main HDO reactions ($C_{aromatic}$−O bond breaking) take place over similar active sites that deactivate roughly at the same rate whereas the transalkylation reaction (guaiacol to cresol reaction) is faster inhibited and may involve different sites than HDO reactions.

The semidetailed kinetic model is embedded into an Aspen Plus simulation, which handles the whole lignin to BTX process including lignin pyrolysis and catalytic HDO and products recovery.

The Aspen Plus model can be used for optimizing the BTX or phenol yield as a function of some process parameters. Mass and carbon balances of the integrated lignin to BTX process are predicted. The important carbon loss during the pyrolysis step and the detrimental effect of the pyrolysis carrier gas are pointed out.

It is stressed that better lignin conversion technologies should be looked for to increase the yield in monoaromatic compounds at the expense of char and lignin oligomers and to decrease the amount of carrier gas. The coproduction of hydrocarbons with solid carbons (such as activated carbon or fibers) and syngas should also be addressed for a technical-economical optimization of lignin valorization.

■ AUTHOR INFORMATION

Corresponding Author
*E-mail: Anthony.dufour@univ-lorraine.fr.

Notes
The authors declare no competing financial interest.

■ REFERENCES

(1) Holladay, J.; Bozell, J.; White, J.; Johnson, D. *Top Value-Added Chemicals from Biomass Vol. II—Results of Screening for Potential Candidates from Biorefinery Lignin*; U.S. Department of Energy: Washington, DC, 2007.

(2) Huber, G. W.; Iborra, S.; Corma, A. *Chem. Rev.* **2006**, *106*, 4044−4098.

(3) Haveren, J.; Scott, E. L.; Sanders, J. *Biofuels, Bioprod. Biorefin.* **2008**, *2*, 41−57.

(4) Zakzeski, J.; Bruijnincx, P. C. A.; Jongerius, A. L.; Weckhuysen, B. M. *Chem. Rev.* **2010**, *110*, 3552−3599.

(5) Rodriguez-Mirasol, J.; Cordero, T.; Rodriguez, J. J. *Energy Fuels* **1993**, *7*, 133−138.

(6) Kadla, J. F.; Kubo, S.; Venditti, R. A.; Gilbert, R. D.; Compere, A. L.; Griffith, W. *Carbon* **2002**, *40*, 2913−2920.

(7) Shabtai, J. S.; Zmierczak, W. W.; Chornet, E.; Johnson, D. Process for converting lignins into a high octane blending component. U.S. Patent No. US20030115792, 2003.

(8) Ma, Z.; Troussard, E.; Van Bokhoven, J. A. *Appl. Catal., A* **2012**, *423-424*, 130−136.

(9) Rødsrud, G.; Lersch, M.; Sjöde, A. *Biomass Bioenergy* **2012**, *46*, 46−59.

(10) De Wild, P. In *PyNE IEA Bioenergy Task 34 Newsletter 29*; Aston University Bioenergy Research Group: Birmingham, U.K., 2011.

(11) Goheen, D. *Adv. Chem.* **1966**, *59*, 205−225.

(12) Effendi, A.; Gerhauser, H.; Bridgwater, A. V. *Renewable Sustainable Energy Rev.* **2008**, *12*, 2092−2116.

(13) Green Car Congress: Mascoma Announces Feedstock Processing and Lignin Supply Agreement with Chevron Technology Ventures; Chevron Working on Converting Lignin to Hydrocarbon Fuel Components. http://www.greencarcongress.com/2009/09/mascoma-chevron.html (accessed July 17, 2012).

(14) Parkhurst, H.; Huibers, D.; Jones, M. In *Symposium on Alternate Feedstocks for Petrochemicals, ACS San Francisco Meeting*; American Chemical Society: Washington, DC, 1980; pp 657−667.

(15) Mullen, C. A.; Boateng, A. A. *Fuel Process. Technol.* **2010**, *91*, 1446−1458.

(16) Snell, G. J.; Huibers, D. T. A. Lignin cracking process using fast fluidized bed reactions. U.S. Patent No. US4409416, 1983.

(17) De Wild, P.; Van der Laan, R.; Kloekhorst, A.; Heeres, E. *Environ. Prog. Sustainable Energy* **2009**, *28*, 461−469.

(18) Briens, C. In *The International Conference on Thermochemical Conversion Science*; Chicago, 2011.

(19) Olcese, R. N.; Bettahar, M.; Petitjean, D.; Malaman, B.; Giovanella, F.; Dufour, A. *Appl. Catal., B* **2012**, *115−116*, 63−73.

(20) Olcese, R. N.; Bettahar, M. M.; Malaman, B.; Ghanbaja, J.; Tibavisco, L.; Petitjean, D.; Dufour, A. *Appl. Catal., B* **2013**, *129*, 528−538.

(21) Gonzalez-Borja, M. A.; Resasco, D. E. *Energy Fuels* **2011**, *25*, 4155−4162.

(22) Shin, E.-J.; Keane, M. A. *Ind. Eng. Chem. Res.* **2000**, *39*, 883−892.

(23) Zhao, H. Y.; Li, D.; Bui, P.; Oyama, S. T. *Appl. Catal., A* **2011**, *391*, 305−310.

(24) Zhu, X.; Lobban, L. L.; Mallinson, R. G.; Resasco, D. E. *J. Catal.* **2011**, *281* (1), 21−29.

(25) Pindoria, R. .; Megaritis, A.; Herod, A. .; Kandiyoti, R. *Fuel* **1998**, *77*, 1715−1726.

(26) Dufour, A.; Castro-Diaz, M.; Marchal, P.; Brosse, N.; Olcese, R.; Bouroukba, M.; Snape, C. E. *Energy Fuels* **2012**, *26*, 6432−6441.

(27) Lédé, J.; Broust, F.; Ndiaye, F. T.; Ferrer, M. *Fuel* **2007**, *86*, 1800−1810.

(28) Jendoubi, N.; Broust, F.; Commandre, J. M.; Mauviel, G.; Sardin, M.; Lédé, J. *J. Anal. Appl. Pyrolysis* **2011**, *92*, 59−67.

(29) Bui, V. N.; Laurenti, D.; Delichere, P.; Geantet, C. *Appl. Catal., B* **2010**, *101*, 246−255.

(30) Bui, V. N.; Laurenti, D.; Afanasiev, P.; Geantet, C. *Appl. Catal., B* **2011**, *101*, 239−245.

(31) Bui, V. N.; Toussaint, G.; Laurenti, D.; Mirodatos, C.; Geantet, C. *Catal. Today* **2009**, *143*, 172−178.

(32) Zhu, X.; Mallinson, R. G.; Resasco, D. E. *Appl. Catal., A* **2010**, *379*, 172−181.

(33) Aho, A.; Kumar, N.; Lashkul, A.; Eränen, K.; Ziolek, M.; Decyk, P.; Salmi, T.; Holmbom, B.; Hupa, M.; Murzin, D. Y. *Fuel* **2010**, *89*, 1992−2000.

(34) Valle, B.; Gayubo, A. G.; Aguayo, A. T.; Olazar, M.; Bilbao, J. *Energy Fuels* **2010**, *24*, 2060−2070.

(35) Nimmanwudipong, T.; Runnebaum, R. C.; Block, D. E.; Gates, B. C. *Energy Fuels* **2011**, *25*, 3417−3427.

(36) Groot, C. K.; De Beer, V. H. J.; Prins, R.; Stolarski, M.; Niedzwiedz, W. S. *Ind. Eng. Chem. Prod. Res. Dev.* **1986**, *25*, 522−530.

(37) Antonakou, E.; Lappas, A.; Nilsen, M. H.; Bouzga, A.; Stöcker, M. *Fuel* **2006**, *85*, 2202−2212.

(38) Abdelouahed, L.; Authier, O.; Mauviel, G.; Corriou, J. P.; Verdier, G.; Dufour, A. *Energy Fuels* **2012**, *26* (6), 3840−3855.

(39) François, J.; Abdelouahed, L.; Mauviel, G.; Feidt, M.; Mirgaux, O.; Rogaume, C.; Patisson, F.; Dufour, A. In *4th International Conference on Engineering for Waste and Biomass Valorisation*; Porto, Portugal, 2012.

(40) Faravelli, T.; Frassoldati, A.; Migliavacca, G.; Ranzi, E. *Biomass Bioenergy* **2010**, *34*, 290−301.

(41) Sharma, R. K.; Wooten, J. B.; Baliga, V. L.; Lin, X.; Geoffrey Chan, W.; Hajaligol, M. R. *Fuel* **2004**, *83*, 1469−1482.

(42) Scholze, B.; Meier, D. *J. Anal. Appl. Pyrolysis* **2001**, *60*, 41−54.

(43) Spath, P.; Aden, A.; Eggeman, T.; Ringer, M.; Wallace, B.; Jechura, J. *Biomass to Hydrogen Production Detailed Design May 2005 and Economics Utilizing the Battelle Columbus Laboratory Indirectly-Heated Gasifier*; U.S. National Renewable Energy Laboratory: Golden, CO, 2005.

(44) Elliott, D. *PyNe IEA Bioenergy Task 34 Newsletter 30*; Aston University Bioenergy Research Group: Birmingham, U.K., 2011.

(45) Franck, H.-G.; Franck, H.-G.; Stadelhofer, J. W. *Industrial Aromatic Chemistry: Raw Materials, Processes, Products*; Springer-Verlag: Berlin, 1988.

(46) Farmer, J. *Benzene Emission from Coke by-Product Recovery Plants—Background Information for Proposed Standards*; U.S. Environmental Protection Agency: Washington, DC, 1984.

(47) Mihalcik, D. J.; Boateng, A. A.; Mullen, C. A.; Goldberg, N. M. *Ind. Eng. Chem. Res.* **2011**, *50*, 13304−13312.

(48) Silva, T. C. F.; Santos, R. B.; Jameel, H.; Colodette, J. L.; Lucia, L. A. *Energy Fuels* **2012**, *26*, 1315−1322.

(49) Carlson, T. R.; Cheng, Y.-T.; Jae, J.; Huber, G. W. *Energy Environ. Sci.* **2011**, *4*, 145.

(50) Poling, B. E.; Prausnitz, J. M.; John Paul, O. C. *The Properties of Gases and Liquids*; McGraw-Hill: New York, 2001; Vol. 5.

(51) Dufour, A.; Celzard, A.; Ouartassi, B.; Broust, F.; Fierro, V.; Zoulalian, A. *Appl. Catal., A* **2009**, *360*, 120−125.

(52) LaVopa, V.; Satterfield, C. N. *Energy Fuels* **1987**, *1*, 323−331.

(53) Furimsky, E. *Appl. Catal., A* **2000**, *199*, 147−190.

(54) Marín-Astorga, N.; Pecchi, G.; Fierro, J. L. G.; Reyes, P. *J. Mol. Catal. A: Chem.* **2005**, *231*, 67−74.

(55) Forzatti, P.; Lietti, L. *Catal. Today* **1999**, *52*, 165−181.

(56) Olcese, R. N.; Carre, V.; Aubriet, F.; Dufour, A. *Energy Fuels* **2013** submitted for publication.

(57) Geldart, D. *Powder Technol.* **1973**, *7*, 285−292.

(58) Nowakowski, D. J.; Bridgwater, A. V.; Elliott, D. C.; Meier, D.; De Wild, P. *J. Anal. Appl. Pyrolysis* **2010**, *88*, 53−72.